

Oxygen reduction at platinum nanoparticles supported on carbon cryogel in alkaline solution

N. R. ELEZOVIĆ^{1*#}, B. M. BABIĆ², L.J. M. VRAČAR^{3#} and N. V. KRSTAJIĆ³

¹Center for Multidisciplinary Studies, University of Belgrade, P.O. Box 33, Belgrade, ²Vinča Institute of Nuclear Sciences, P.O. Box 522, 11001 Belgrade and ³Faculty of Technology and Metallurgy, University of Belgrade, Belgrade, Serbia

(Received 19 October 2006, revised 17 January 2007)

Abstract: The oxygen reduction reaction was investigated in 0.1 M NaOH solution, on a porous coated electrode formed of Pt particles supported on carbon cryogel. The Pt/C catalyst was characterized by the X-ray diffraction (XRD), transmission electron microscopy (TEM) and cyclic voltammetry techniques. The results demonstrated a successful reduction of Pt to metallic form and homogenous Pt particle size distribution with a mean particle size of about 2.7 nm. The ORR kinetics was investigated by linear sweep polarization at a rotating disc electrode. The results showed the existence of two $E - \log j$ regions, usually referred to polycrystalline Pt in acid and alkaline solution. At low current densities (lcd), the Tafel slope was found to be close to $-2.3RT/F$, while at high current densities (hcd) it was found to be close to $-2 \times 2.3RT/F$. It is proposed that the main path in the ORR mechanism on Pt particles was the direct four-electron process, with the transfer of the first electron as the rate determining step. If the activities are expressed through the specific current densities, a small enhancement of the catalytic activity for Pt/C was observed compared to that of polycrystalline Pt. The effect of the Pt particle size on the electrocatalysis of oxygen reduction was ascribed to the predominant (111) facets of the platinum crystallites.

Keywords: oxygen reduction reaction, Pt nanoparticles, carbon support, alkaline solutions

INTRODUCTION

The oxygen reduction reaction is one of the most important electrochemical reactions because it is the cathodic reaction in fuel cells and metal air batteries, during aerated media corrosion and in some industrial electrolytic processes. For these reasons, research efforts have been focused on developing a proper catalyst and elucidating the mechanism of this reaction.^{1–8} Platinum and platinum alloys are, in spite of efforts to replace them, still the best known electrocatalysts for the oxygen reduction reaction, since they have a high catalytic activity and chemical

* Corresponding author. E-mail: nelezovic@tmf.bg.ac.yu

Serbian Chemical Society member.

doi: 10.2298/JSC0707699E

stability. Nowadays, researchers are mostly dealing with precious metals, mainly platinum and its alloys, dispersed on high surface area carbon, and their efforts are concentrated on the reduction of the amount of Pt.^{9,10}

The electrochemical oxygen reduction reaction has been extensively studied in acid solutions, due to its application in fuel cells with a proton exchange membrane. However, there are few works in alkaline solution,^{11–13} especially on platinum nanoparticles.^{14,15} According to many authors, the electrochemical reduction of oxygen on Pt occurs by the parallel mechanism with predominantly direct four-electron reduction, even in alkaline solutions. The steady state kinetics in acid solution is characterized by two linear Tafel slopes: $-2.3RT/F$ at low current densities and $-2 \times 2.3RT/F$ at high current densities. The change in Tafel slopes is, generally, a consequence of a change in the rate determining steps (rds). However, many workers agreed that the different Tafel slopes arose from different adsorption conditions of the reaction intermediates in these two cd regions and that the same first charge transfer step was the rds in both current densities regimes.^{2,16–18}

In this study the oxygen reduction reaction was investigated on a Pt/C electrode in alkaline electrolyte and results are compared to those on polycrystalline Pt. Namely, the development of alkaline anion exchange membranes is well advanced^{19,20} and such membranes will enable the benefits of the kinetics of the oxygen reduction reaction in alkaline solutions to be employed.

EXPERIMENTAL

Carbon support and catalyst preparation

Home made carbon cryogel synthesized by sol–gel polycondensation and freeze-drying with a specific surface area (BET) of $517 \text{ m}^2 \text{ g}^{-1}$ was used as a catalyst support.²¹ The Pt was deposited on the support by a modified ethylene glycol method.²²

Electrode preparation

The catalyst ink was prepared using one milligram of Pt/C catalyst ultrasonically suspended in 1.0 ml of a water–methanol mixture (v/v : 1/1) and 50 μl of Nafion solution (5 wt. % solution, Aldrich). Then 12.5 μl of ink was transferred by an injector to a clean gold disk electrode (6 mm diameter, with area of 0.28 cm^2). After volatilization of the water–methanol, the electrode was heated at $80 \text{ }^\circ\text{C}$ for 10 min.

Characterization of the catalyst

X-Ray diffraction (XRD) analysis, performed on a Siemens D500 X-ray diffractometer using $\text{CuK}\alpha$ radiation with a Ni filter, was used for the characterization of the Pt/C catalyst powder. The 2θ angular regions between 5 and 70° were explored at a scan rate of $0.02^\circ \text{ s}^{-1}$ with an angular resolution of 0.02° for all XRD tests.

Transmission electron microscopy (TEM) measurements were performed at the National Center for Electron Microscopy (NCEM)²³ using a PEI Phillips instrument. The suspension for transmission electron microscopy, prepared from catalyst powder and ethanol, was dropped onto a clean holey carbon grid and dried in air. The particle size distribution was determined from images of, on average, 20 different regions containing 10 – 20 particles each. The particle shape was determined

by real space crystallography using high-resolution images taken from particles near or on the edge of the carbon black substrate and/or by numerical Fourier filtering of the digitized image intensity spectrum of particles on the top of the carbon.

Electrochemical characterization

A conventional RDE three-compartment all-glass cell was used. The counter electrode was a platinum sheet of 5 cm² geometric area. A reversible hydrogen electrode, in the same solution, was used as the reference electrode. The working electrode used in this study was in the form of a rotating disk. The experiments were performed at 25 °C. The electrolytes were 0.1 M NaOH and 0.1 M HClO₄ prepared with highly pure water.

The experiments were performed by the potentiodynamic method. A PAR Universal Programmer, Model 175, was used to provide potentiodynamic voltage–time program addressed to a PAR Model 371 Potentiostat/Galvanostat.

RESULTS AND DISCUSSION

XRD and TEM characterization of the catalyst

The XRD results²⁴ showed three characteristic reflection peaks in all spectra: the peak at $2\theta = 44.2^\circ$ corresponds to the hexagonal graphite structure (100) and the diffraction peaks at about 39° , 46° and 68° correspond to the Pt (111), (200) and (220) planes, respectively. The first peak suggests good graphite characteristics of the carbon cryogel and the diffraction peaks of the fcc Pt demonstrate a successful reduction of the Pt precursor to the metallic form and it represents the typical character of a crystalline Pt face that is in the face-centered cubic (fcc) phase. As there are no other distinct peaks in the investigated 2θ range than the three Pt peaks mentioned above, it can be concluded that all the in-house supported Pt catalysts had a prevailing Pt (fcc) crystal structure.

TEM Micrograph shows very uniform size distribution of the Pt nanoparticles (Fig. 1a), with a mean particle size of about 2.7 nm for the supported Pt catalyst. The atomically resolved image in Fig. 1b shows Pt lattice planes with a spacing corresponding to the (200) and (111) planes of the face-centered cubic Pt nanoparticles, as was indicated in the relevant digital diffractogram. The Pt particles have common cubo-octahedral shapes. Occasionally, twinned particles were observed with the same (111) twinning plane as in some other Pt-based catalysts.²³

Cyclic voltammetry analysis

The cyclic voltammograms obtained at a Pt/C electrode in N₂ saturated 0.5 M HClO₄ and in N₂ saturated 0.1 M NaOH solutions, performed to determine the electrochemically active surface area and to compare the adsorption properties of the catalyst in acid and alkaline solutions, are presented in Fig. 2a and Fig. 2b, respectively. The double layer region in the alkaline solution was not well-defined as in the acid solution, which was also found for Pt single crystal electrodes.¹¹ The voltammograms in both acid and alkaline solutions also indicate

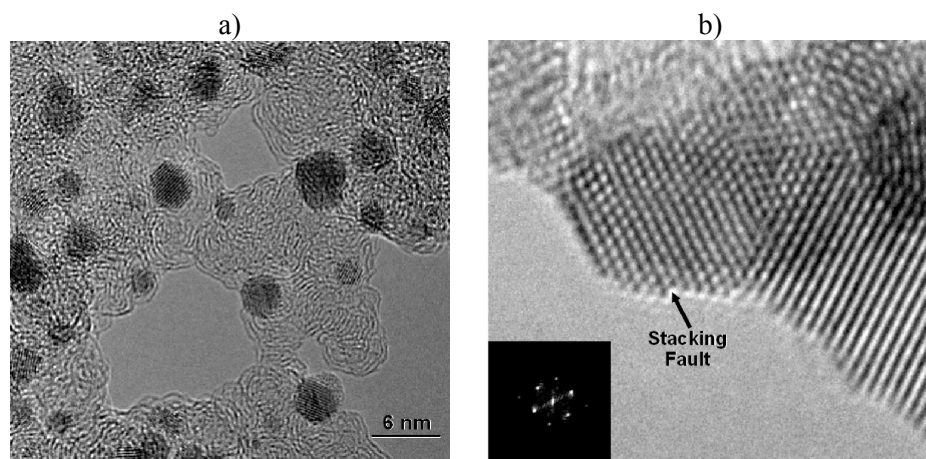


Fig. 1. TEM Images of Pt nanoparticles on carbon substrate. a) An overview showing the distribution of the sizes of the Pt particles on carbon support; b) high resolution image showing a cubo-octahedral shape of Pt particle.

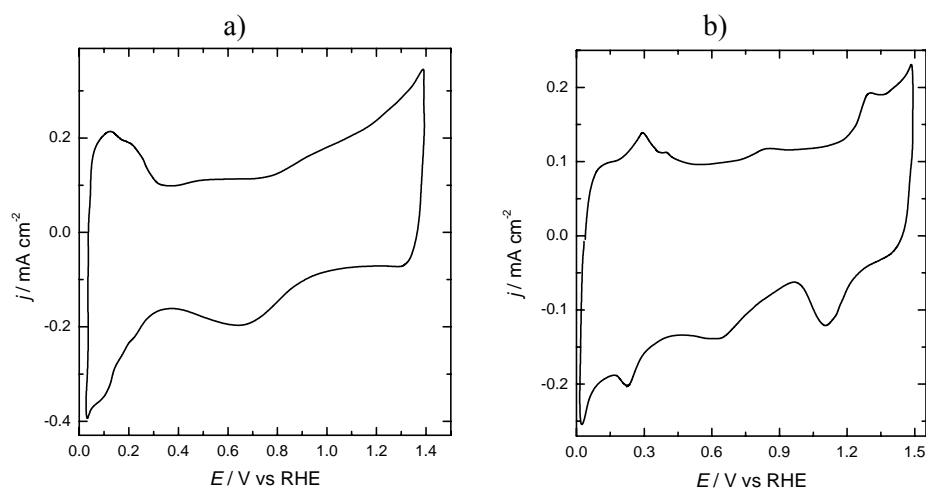


Fig. 2. Cyclic voltammetry curves for Pt/C in: a) N_2 saturated 0.5 M HClO_4 solution and b) N_2 saturated 0.1 M NaOH , at a sweep rate of 100 mV s^{-1} .

that there are some differences in the features of the hydrogen desorption process, with respect to those of polycrystalline Pt. In the acid solution, the hydrogen oxidation peak, corresponding to the desorption of the hydrogen atoms from the edge and corner sites of the platinum crystallites, was pronounced^{25–27} and this could be attributed to the fact that small platinum particles show an increased number of edge and corner sites, which is a consequence of the change of the fraction of the atomic surface of the (111) and (100) faces.²⁶ This is consistent with

the fact that for smaller particles, the fraction of the atomic surface of Pt atoms in the (111) face is higher than those for the other orientations.²⁶ The unclear separation of the hydrogen, oxygen and double layer regions in alkaline solution is a consequence of the fact that the adsorption of oxygen-containing species on different Pt facets starts at potentials close to the hydrogen region. This is the reason why the anodic part of the CV curve is not fully parallel with the potential axis in the conventional double layer region. As a consequence of all this, the desorption charge of hydrogen atoms, after extraction of the double layer charge, was found to be lower in the alkaline solution, as was already reported in the literature.¹² On account of these differences, the real electrode surface area of the Pt catalyst was determined by integrating the charge under the hydrogen desorption curve in acid solution (Fig. 2a), taking the reference value of $210 \mu\text{C cm}^{-2}$ for full coverage with adsorbed hydrogen species.²⁸ This calculation gave the value of $68 \text{ m}^2 \text{ g}^{-1}$ for Pt/C electrode.

Kinetics of the oxygen reduction reaction

The rotating disk electrode measurements of the ORR in 0.1 M NaOH were performed to test the catalytic activity of the Pt/C catalyst and compare it with that of polycrystalline Pt. The rotating disk electrode voltammogram of Pt/C in O_2 -saturated NaOH solution, at a sweep rate of 20 mV s^{-1} , as a function of the rotation rate is shown in Fig. 3. It can be seen that the onset of the ORR and the half-wave potential were significantly shifted to more positive potentials in the case of the Pt/C electrode, indicating its higher catalytic activity for the reduction of oxygen, compared to that of polycrystalline Pt (Fig. 4). For a mixed control process, the activation and mass-transport controlled current densities are combined to yield the total current density as the sum of reciprocals:

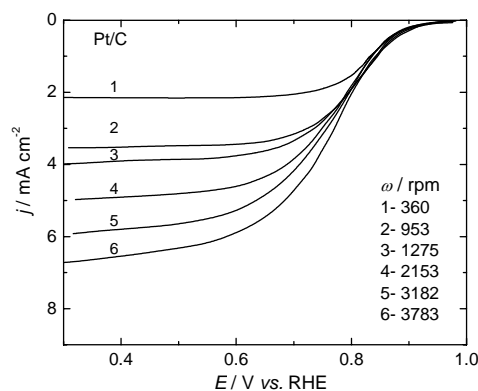


Fig.3. Polarization curves obtained with a rotating disk electrode for O_2 reduction in 0.1 M NaOH solution at Pt/C electrode, at sweep rate of 20 mV s^{-1} .

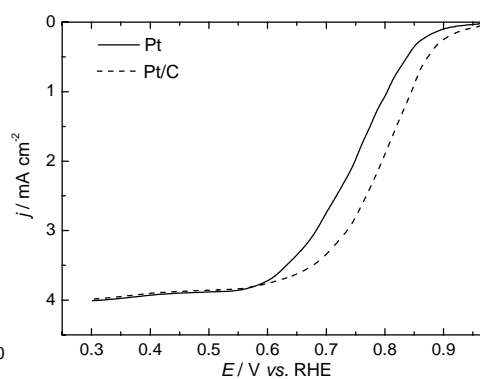


Fig.4. Polarization curves for O_2 reduction on Pt and Pt/C in 0.1 mol dm^{-3} NaOH solution, at a rotating speed of 1280 rpm, with sweep rate of 20 mV s^{-1} .

$$\frac{1}{j} = \frac{1}{j_k} + \frac{1}{B\omega^{1/2}} \quad (1)$$

where j is the measured current density, j_k is the activation controlled current density, ω is the rotation rate of the electrode and B is the Levich slope, the theoretical value of which is given by the Equation:

$$B = 0.62 n F C(\text{O}_2) D_{\text{O}_2}^{2/3} \nu^{-1/6} \quad (2)$$

where: n is the number of electrons transferred per oxygen molecule, F is the Faraday constant, D_{O_2} is the diffusion coefficient of oxygen ($2.22 \times 10^{-5} \text{ cm}^2 \text{ s}^{-1}$), ν is the kinematics viscosity of the solution ($1.1 \times 10^{-2} \text{ cm}^2 \text{ s}^{-1}$) and $C(\text{O}_2)$ is the bulk concentration of oxygen molecules ($1.13 \times 10^{-6} \text{ mol cm}^{-3}$). The values of these coefficients are referred to a 0.1 mol dm^{-3} NaOH solution.²⁹

From the Koutecky–Levich plots (Eq. (1)), the kinetic currents of oxygen reduction can be calculated from the intercepts of the j^{-1} vs. $\omega^{-1/2}$ lines. From the slopes of the lines, the constant B and the number of the electrons exchanged in the reduction can be obtained.

The I^{-1} vs. $\omega^{-1/2}$ plots at different potentials for the Pt/C electrode are presented in Fig. 5. These plots are parallel, indicating first order kinetics with respect to molecular oxygen.³⁰ The slope of these plots gives the value of constant $B = 0.021 \text{ mA rpm}^{-1/2}$. This value is in good agreement with the theoretical value of $0.019 \text{ mA rpm}^{-1/2}$ calculated for a four-electron reduction of oxygen in 0.1 mol dm^{-3} NaOH solution.

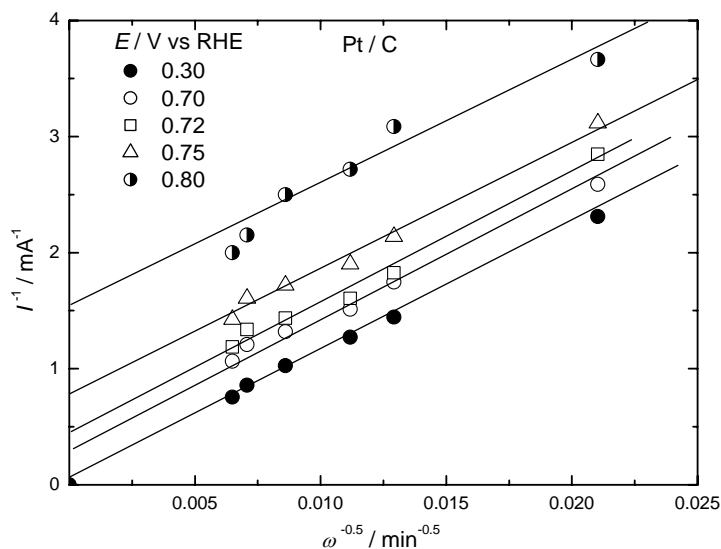


Fig. 5. Koutecky–Levich plots for Pt/C electrode at different potentials, obtained from the data in Fig. 3.

The Tafel plots for Pt/C and polycrystalline Pt, obtained from the kinetic currents, are presented in Fig. 6. The current densities were normalized to the electrochemical active surface area (for the polycrystalline Pt, the experimentally determined roughness factor of 2.5 was used). Both electrodes are characterized by two Tafel slopes: one close to $-2.3 \times 2RT/F$ at high current densities and the other close to $-2.3RT/F$ at low current densities, usually referenced for polycrystalline Pt in alkaline solution.¹¹

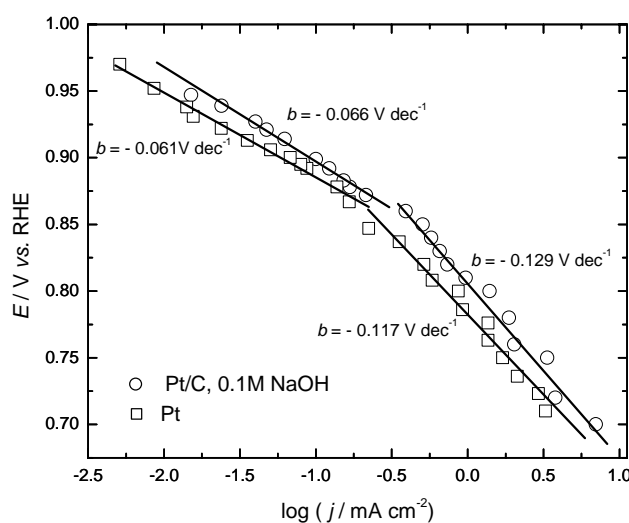


Fig. 6. Tafel plots normalized to the electrochemically active surface area for O_2 reduction in 0.1 M NaOH solution at Pt and Pt/C electrodes.

These results show that the kinetics of oxygen reduction on the Pt/C electrode in alkaline solution is described by the same Equations as those on Pt, and also that the four-electron reduction mechanism, with the first charge transfer rate as the rate determining step, is operative over the whole range of potential.

The existence of two slopes for both electrodes could be explained in terms of the coverage of the electrode surface by adsorbed oxygen species, which follows a Temkin isotherm in the low current density region and a Langmuir isotherm in the higher current density region, meaning that the adsorption conditions are the same on both electrodes.

Based on literature data,^{1-3,9} the ORR on platinum in aqueous solutions has generally been explained by a mechanism involving two parallel paths: in the main one, oxygen is reduced directly to OH^- by a four-electron transfer and in the second one, HO_2^- is first formed by a two-electron transfer process, followed by its further reduction. Numerous investigations of the ORR were performed using of rotating ring-disk electrode, because it is practically the only reliable way to propose the mechanism of the ORR. Therefore, Koutecky–Levich analy-

sis presents an alternate way to rotating ring-disk electrode measurements in the analysis of the actual reaction path. On the basis of this analysis, according to the number of electrons exchanged, the direct four electron mechanism, or at least that the reduction of H_2O_2 is a very fast process, can be proposed.

Lima and Ticianelli³¹ reported that the four electron mechanism predominates for Pt/C catalysts with more than 20 % of platinum on carbon. The same conclusion was drawn by Genies *et al.*,¹³ who proved that oxygen reduction on carbon was mainly a two-electron process but that on platinum particles, the importance of this path was so small that it was difficult to be fully characterized by RRDE experiments.

The comparison of the specific activities of Pt/C and Pt electrodes for the ORR (Fig. 6) reveals a small enhancement of the catalytic activity for Pt/C. This result seems to be related to the weak adsorption of oxygenated species on the small particles, as the effect of corner and edge atoms, the proportion of which increases for small particles. The present results are in agreement with the results of Markovic *et al.*,³² who also showed that, the Pt (111) face is the most active for the OOR in alkaline solution. Since the proportion of (111) vs. (100) increases for smaller particles, they predicted a slight increase in activity for these particles.

CONCLUSIONS

A highly dispersed carbon supported Pt catalyst with a loading of 20 wt. % Pt was successfully synthesized. Comparison with polycrystalline Pt showed a slight enhancement in the catalytic activity for the oxygen reduction reaction, expressed through the electrochemically active surface area. Kinetics and mechanism of the reaction at Pt/C catalyst were found to be the same as in a case of polycrystalline Pt. The results presented above did not show a promising increase in the specific catalytic activity but illustrated that Pt nanoparticles supported on carbon cryogel can be employed as a catalyst for the ORR.

Acknowledgement: The authors are indebted to the Ministry of Science and Environment Protection Republic of Serbia for the financial support of this work under the Contract number 142038

ИЗВОД

ЕЛЕКТРОХЕМИЈСКА РЕАКЦИЈА РЕДУКЦИЈЕ КИСЕОНИКА НА НАНОЧЕСТИЦАМА ПЛАТИНЕ НА УГЉЕНИЧНОМ НОСАЧУ У АЛКАЛНОМ РАСТВОРУ

Н. Р. ЕЛЕЗОВИЋ¹, Б. М. БАБИЋ², Ј. М. ВРАЧАР³ и Н. В. КРСТАЈИЋ³

¹Центар за мултидисциплинарне студије Универзитета у Београду, Београд, ²Институт за нуклеарне науке "Винча", Београд и ³Технолошко-металуришки факултет Универзитета у Београду, Србија

Кинетика реакције редукције кисеоника је испитивана на наночестицама платине диспергованим на угљеничном носачу, у 0.1 mol dm^{-3} NaOH, на 25 °C. За синтезу Pt катализатора (Pt/C) је примењена модификована полиол метода из раствора етилен гликола, док је као носач коришћен угљенични криогел. Тако добијени катализатор је окарактерисан применом ВЕТ методе, дифракције X-зрака (XRD) и трансмисионе електронске микроскопије (ТЕМ).

Добијени резултати су показали веома хомогену расподелу наночестица Pt, са просечном величином честица око 2,7 nm. За испитивање кинетике реакције редукције кисеоника су коришћене стационарна поларизациона метода и метода цикличне волтаметрије. Показано је да област малих густина струје на кривој поларизације карактерише вредност Тафеловог нагиба око -60 mV dek^{-1} , док је у области већих густина струје ова вредност блиска -120 mV dek^{-1} . Према дојеним резултатима, главни реакциони пут у механизму редукције кисеоника је директна четвороелектронска измена, при чему је ступањ који одређује укупну брзину реакције пренос првог електрона. Поређењем каталитичке активности, изражене преко густине струје по реалној површини катализатора, констатована је нешто већа активност Pt/C катализатора у односу на поликристалну Pt, што је последица доминације (111) равни у кристалној структури дисперговане платине.

(Примљено 19. октобра 2006, ревидирано 17. јануара 2007)

REFERENCES

1. S. Gottsfeld, T. A. Zawodzinski, *Advances in Electrochemical science and Engineering*, R. C. Alkire, D. M. Kolb, Eds., Vol. 5, Wiley-VCH, Weinheim (1997)
2. M. R. Tarasevich, *Elektrokhimiya* **9** (1973) 599
3. P. N. Ross, *J. Electrochem. Soc.* **126** (1979) 78
4. D. B. Šepa, M. V. Vojnović, A. Damjanović, *Electrochim. Acta* **25** (1980) 1491
5. D. B. Šepa, M. V. Vojnović, Lj. M. Vračar, A. Damjanović, *Electrochim. Acta* **31** (1986) 91
6. T. J. Schmidt, V. Stamenković, M. Arenz, N. M. Marković, P. N. Ross, *Electrochim. Acta* **47** (2002) 3765
7. M. D. Obradović, B. N. Grgur, Lj. M. Vračar, *J. Electroanal. Chem.* **548** (2003) 69
8. J. Prakash, H. Joachin, *Electrochim. Acta* **45** (2000) 2289
9. U. A. Paulus, T. J. Schmidt, H. A. Gasteiger, R. J. Behm, *J. Electroanal. Chem.* **495** (2001) 134
10. J. Zhang, Y. Mo, M. B. Vukmirovic, R. Klie, K. Sasaki, R. R. Adzic, *J. Phys. Chem. B* **108** (2004) 10955
11. T. J. Schmidt, V. Stamenkovic, P. N. Ross Jr., N. M. Markovic, *Phys. Chem. Chem. Phys.* **5** (2003) 400
12. K. Tammevski, M. Arulepp, T. Tenno, C. Ferrater, J. Claret, *Electrochim. Acta* **42** (1997) 2961
13. J. Perez, E. R. Gonzalez, E. A. Ticianelli, *Electrochim. Acta* **44** (1998) 1329
14. L. Genies, R. Faure, R. Durand, *Electrochim. Acta* **44** (1998) 1314
15. L. Genies, Y. Bultel, R. Faure, R. Durand, *Electrochim. Acta* **48** (2003) 3879
16. Lj. M. Vračar, N. V. Krstajić, V. R. Radmilović, M. M. Jakšić, *J. Electroanal. Chem.* **587** (2006) 99
17. A. Damjanović, D. B. Šepa, M. V. Vojnović, *Electrochim. Acta* **24** (1979) 887
18. D. B. Šepa, M. V. Vojnović, Lj. M. Vračar, A. Damjanović, *Electrochim. Acta* **32** (1987) 129
19. J. R. Varcoe, R. C. T. Slade, in *Fuel Cells*, Vol. 5, Issue 2, Wiley-VCH, 2005, p.187
20. K. Matsuoka, Y. Iriyama, T. Abe, M. Matsuoka, Z. Ogumi, *J. Power Sources* **150** (2005) 27
21. B. Babić, D. Đokić, N. Krstajić, *J. Serb. Chem. Soc.* **70** (2005) 21
22. B. M. Babic, Lj. M. Vračar, V. Radmilović, N. V. Krstajić, *Electrochim. Acta* **51** (2006) 3820
23. V. Radmilovic, T. J. Richardson, S. J. Chen, P. N. Ross, *J. Catal.* **232** (2005) 99
24. N. R. Elezović, B.M. Babić, N. V. Krstajić, Lj. M. Gajić-Krstajić, Lj. M. Vračar, *Int. J. Hydrogen Energy* (2006) in press
25. G. Tamizhmani, J. P. Dodelet, D. Guay, *J. Electrochem. Soc.* **143** (1996) 18
26. K. Kinoshita, *J. Electrochem. Soc.* **137** (1990) 845
27. S. Mukejee, *J. Appl. Electrochem.* **20** (1990) 537

28. C. H. Hamann, A. Hamnett, W. Vielstich, *Electrochemistry*, Wiley-VCH, 1998, p. 245
29. R. C. Weast, *Handbook of Chemistry and Physics* 55th Ed. R. C West, Cleveland, Oh., 1984.
30. S. Mukejee, S. Srinivasan, *J. Electroanal. Chem.* **350** (1993) 201
31. F. H. B. Lima, E. A. Ticianelli, *Electrochim. Acta* **49** (2004) 4091
32. N. Markovic, H. Gasteiger, P. N. Ross, *J. Electrochem. Soc.* **144** (1997)1591.